Supplemental Figures and Legends

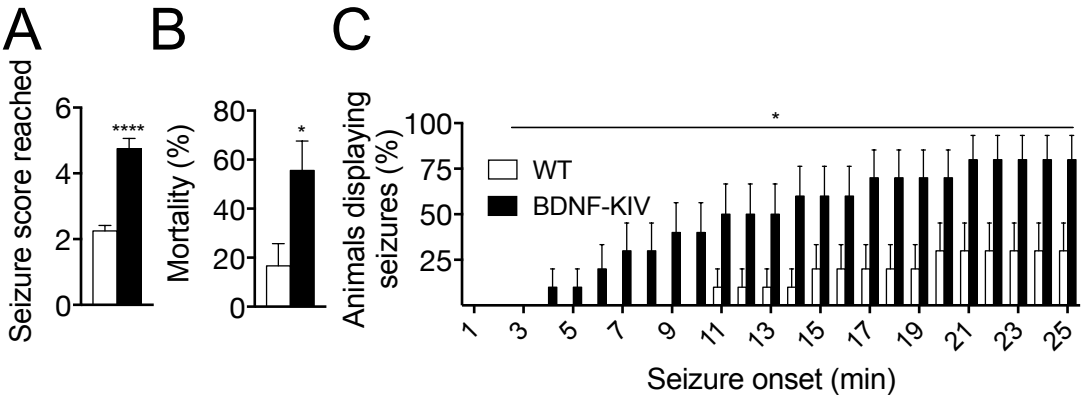

Figure S1. Reduced seizure threshold in BDNF-KIV mice following administration of chemoconvulsants. (A) BDNF-KIV exhibit seizures of increased severity compared to WT (n=8/genotype, *t*-test, p<0.0001) and (B) increased mortality (n=18/group, *t*-test, p=0.0143) following kainic acid administration. (C) Following pentylenetetrazol (PTZ) administration, there is a decreased latency to seize and increased seizure severity in BDNF-KIV mice (n=10/group, 2-way RM ANOVA, genotype difference, p=0.0120, genotype-time interaction, p=0.0029). Data are represented as mean ± standard error of the mean (SEM) (*p<0.05,****p<0.0001).

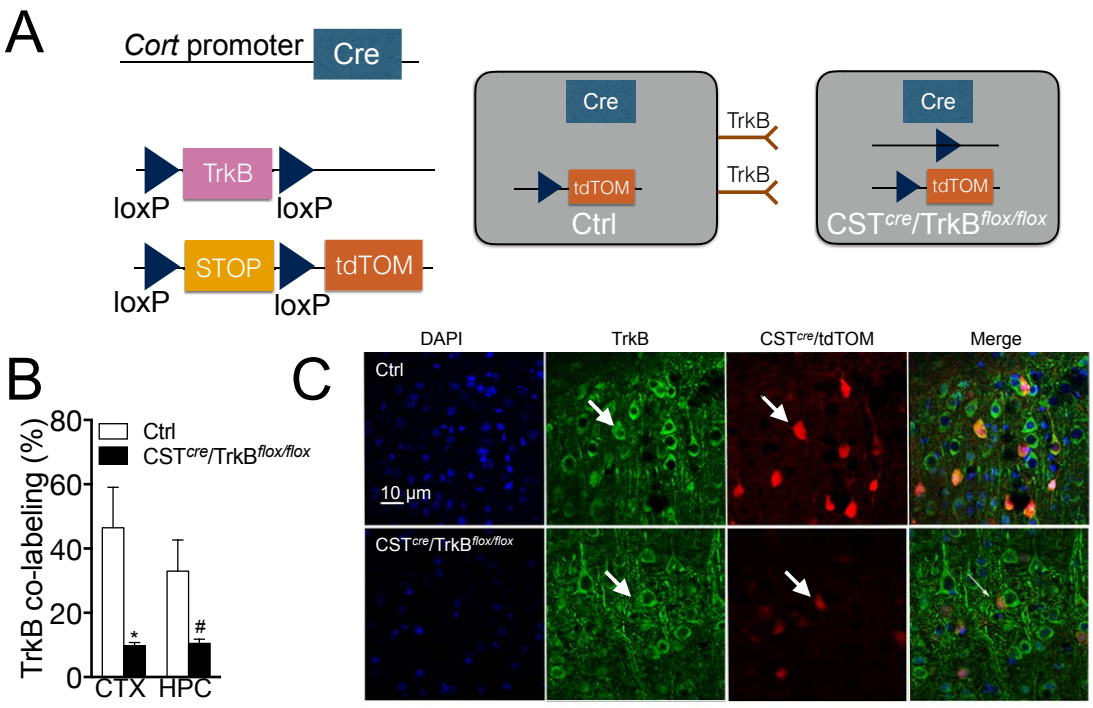

Figure S2. Verification of Tropomyosin Kinase B Receptor (TrkB) deletion in Cortistatin (CST)-positive interneurons. (A) Schematic describing strategy for TrkB deletion and expression of tdTomato (tdTOM) reporter. CST^{cre} mice were crossed to mice with a *loxP*-flanked STOP cassette associated with the TrkB receptor. Mice were additionally crossed to mice expressing a *loxP* flanked STOP cassette in the *Gt(ROSA)26Sor* locus, which prevents transcription of the tdTomato reporter in the absence of Cre-mediated recombination. (B) Immunohistochemical detection of TrkB reveals fewer TrkB expressing tdTOM positive cells in CST^{cre}/TrkB$^{flox/flox}$/tdTOM mice in cortex (CTX) (n=4/group, *t*-test, p=0.0267) and a strong trend towards a difference in the hippocampus (HPC)(*t*-test, p=0.0612) (C) Immunohistochemistry in somatosensory cortex (S1) showing co-labeling of TrkB (green) with tdTOM-labeled CST interneurons (red) in Control (Ctrl) and CST^{cre}/TrkB$^{flox/flox}$/tdTOM mice. For Ctrl, white arrows point to a cell in expressing both tdTOM and TrkB. For CST^{cre}/TrkB$^{flox/flox}$, white arrows point to a cell expressing tdTOM that does not express TrkB. Data are represented as mean ± SEM (*p<0.05, #p<0.07).

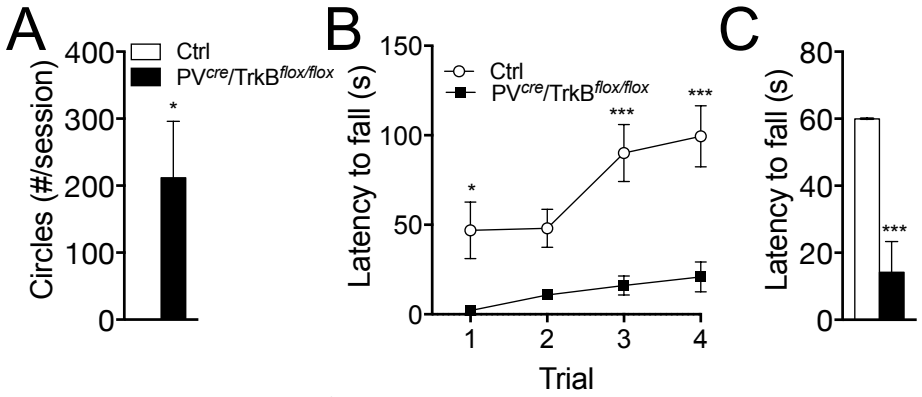

Figure S3. Mice with a selective deletion of the TrkB receptor in parvalbumin (PV) interneurons (PV^{cre}/TrkB$^{flox/flox}$) exhibit motor impairments. (A) PV^{cre}/TrkB$^{flox/flox}$ mice show abnormal circling behavior in an open field (Ctrl: 0.017±0.02, PV^{cre}/TrkB$^{flox/flox}$: 211.7±84.7; *t*-test, p=0.0312). (B) PV^{cre}/TrkB$^{flox/flox}$ mice tested fall off an accelerating rotarod significantly faster than Ctrl (2-way RM ANOVA, genotype difference, p=0.0014, genotype-time interaction, p=0.0134. Post-hoc *t*-test results, trial 1 p<0.05, trial 3 and 4, p<0.0001). (C) Latency to fall in a grip strength wire hanging task was also significantly decreased in PV^{cre}/TrkB$^{flox/flox}$ mice (*t*-test, p=0.0006)(n=6/genotype, all experiments). Data are represented as mean ± SEM (*p<0.05,***p<0.0001).

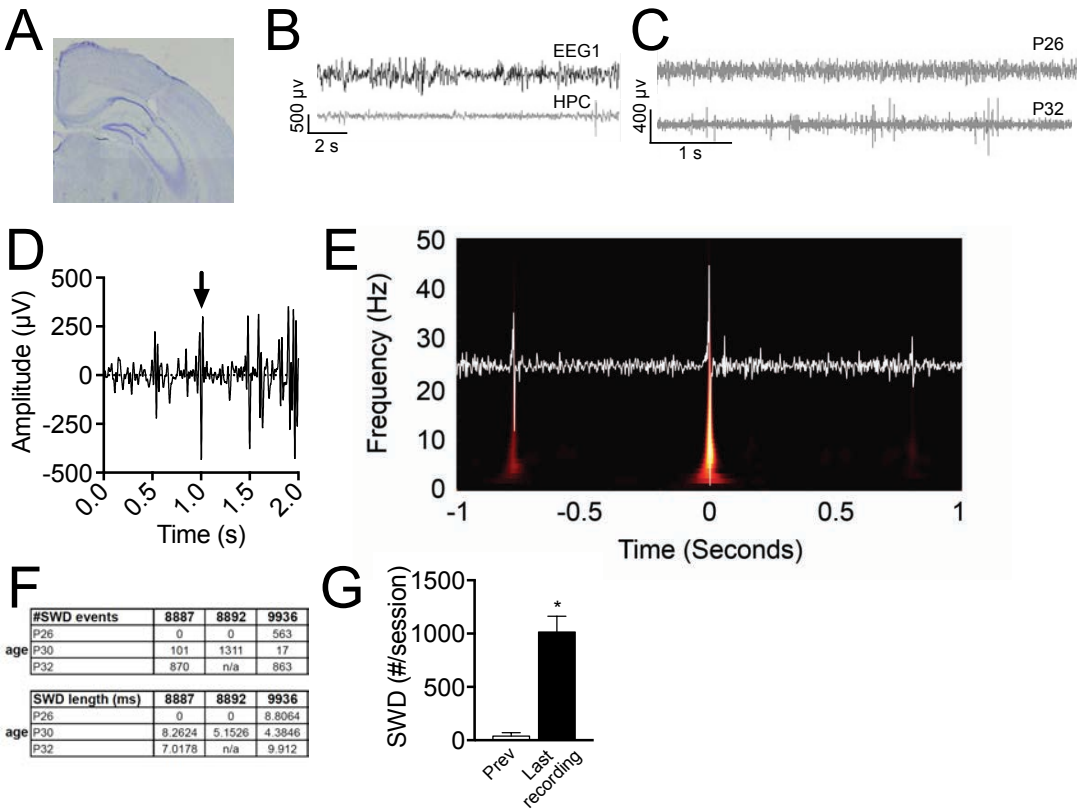

#SWD events	8887	8892	9936
P26	0	0	563
age P30	101	1311	17
P32	870	n/a	863

SWD length (ms)	8887	8892	9936
P26	0	0	8.8064
age P30	8.2624	5.1526	4.3846
P32	7.0178	n/a	9.912

Figure S4. Local field potential (LFP) recorded in HPC of CST^{cre}/TrkB$^{flox/flox}$ mice show sharp wave discharges (SWD). (A) Representative image demonstrating placement of the HPC depth electrode. (B) An example of a seizure in a CST^{cre}/TrkB$^{flox/flox}$ mouse that is detected first in the cortical EEG1 channel, followed by a high amplitude SWD in the HPC channel. (C) HPC data from the same CST^{cre}/TrkB$^{flox/flox}$ mouse at P26 and P32 demonstrates an increase in SWD activity with increasing age and seizure severity. (D) An example of a SWD in a CST^{cre}/TrkB$^{flox/flox}$ mouse identified by automated analysis, centered around SWD onset at 1 s (arrow). (E) Representative spectrogram of SWD data, with the LFP data overlaid in white. (F) Results from SWD analysis for individual animals for the number of events per session at each age, as well as the average length of SWD events for each mouse. A result of n/a is listed to indicate animal death. (G) Bar graph depicting the significant increase in SWD event number for the analyzed CST^{cre}/TrkB$^{flox/flox}$ mice between the final session and the previous session (paired *t*-test, p=0.028). Data are represented as mean ± SEM (*p<0.05).

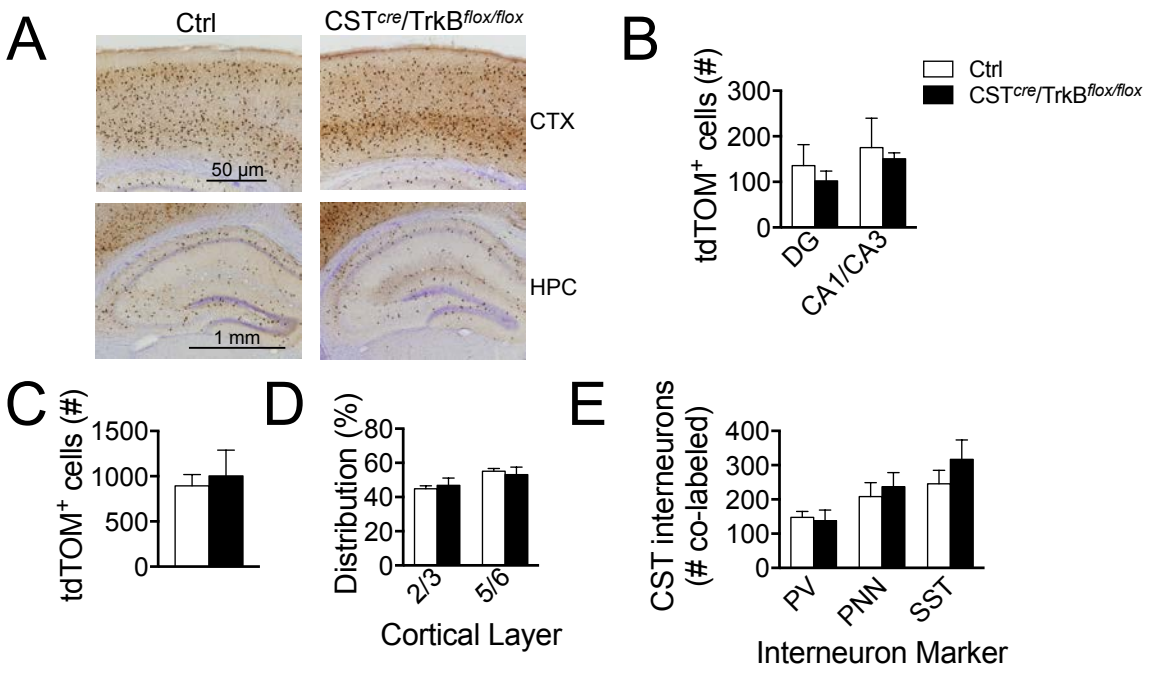

Figure S5. CST cell migration, survival, and excitability are not affected by TrkB deletion. (A) Representative images, captured at 4X magnification demonstrating similar patterns of CST-positive cell expression in the cortex and HPC of Ctrl and CST^{cre}/TrkB$^{flox/flox}$/*tdTOM* mice. (B) Loss of TrkB expression in CST^{cre}/TrkB$^{flox/flox}$/*tdTOM* mice does not alter cell number in HPC subregions dentate gyrus (DG) or CA1/CA3 (DG- *t*-test, p=0.5360; CA1/CA3- *t*-test, p=0.7197). (C) S1 cell counts demonstrate that there is no genotype-dependent difference in the number of tdTOM positive cells (*t*-test, p=0.738) (D) Laminar distribution of CST-interneurons is not altered in CST^{cre}/TrkB$^{flox/flox}$/tdTOM mice (Layer 2/3, *t*-test, p=0.6998; Layer 5/6, *t*-test, p=0.6998)(n=4/group, all counts).(E) No difference in number of CST interneurons co-labeled with parvalbumin (PV), surrounded by a perineuronal net (PNN) or co-labeled with somatostatin (SST) (PV, *t*-test, p=0.7897; PNN, *t*-test, p=0.6439; SST, *t*-test, p=0.3405).

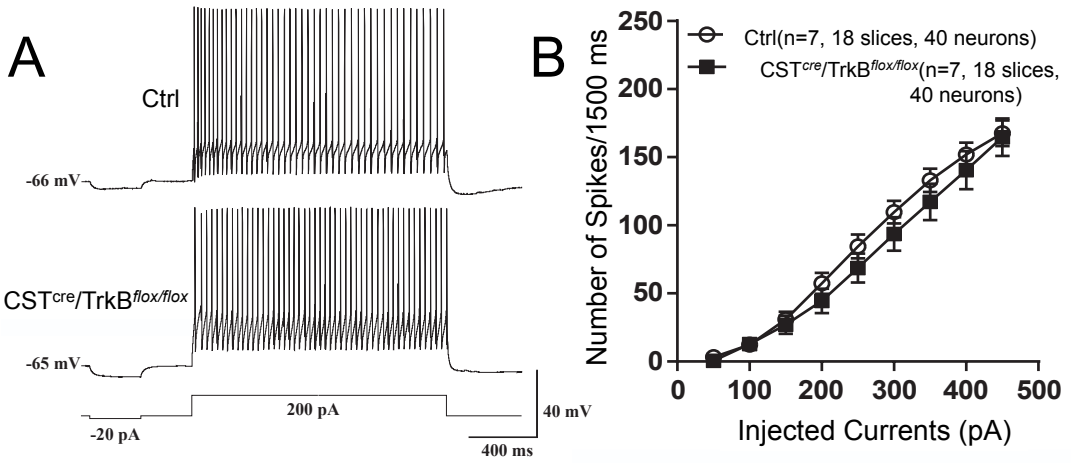

C

Membrane Properties of Layer 2/3 Cortistatin-tdTOM Positive Interneurons in Mouse Somatosensory Cortex			
	Ctrl (n=16)	$CST^{cre}/TrkB^{flox/flox}$ (n=26)	*p* value
Resting Membrane Potential (mV)	-69.97 ± 0.94	-70.14 ± 0.76	0.88
Input Resistance (GΩ)	0.20 ± 0.02	0.16 ± 0.02	0.23
Action Potential Threshold (mV)	-40.08 ± 1.45	-38.18 ± 0.87	0.24
Action Potential Amplitude (mV)	80.63 ± 2.96	82.32 ± 1.82	0.09
Action Potential Half-Width (ms)	1.19 ± 0.13	0.96±0.07	0.33

Figure S6. Excitability and membrane properties of layer 2/3 CST-tdTOM positive interneurons in S1. (A) Representative traces are shown on the upper panel and quantifications on the lower panel. (B) No difference was observed in excitability of mutant cortistatin-tdTOM positive interneurons compared to control. Data are represented as mean ± SEM. (C) Normal membrane properties of layer 2/3 CST-tdTOM positive interneurons in S1 were observed in $CST^{cre}/TrkB^{flox/flox}$ mice, compared with that in Ctrl mice. Action potential threshold was measured at the first point on the rising phase of the spike where the rate of rise exceeded 50 mV/ms. Data are represented as mean ± SEM.

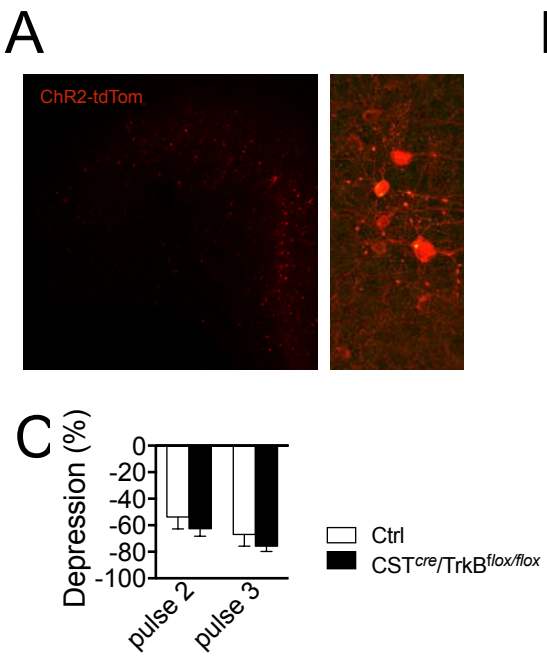

Figure S7. Gamma-aminobutyric acidergic (GABA) transmission from CST-expressing interneurons is preserved in CST^{cre}/TrkB$^{flox/flox}$ mice. (A) Channelrhodopsin-2 (ChR2) was expressed in CST-expressing cells of Ctrl and CST^{cre}/TrkB$^{flox/flox}$ mice by infusing a cre-dependent ChR2:tdTOM virus in cortical layer 2/3. Left, low-magnification image, right, 20X image of infected cells. (B) A representative example of light evoked inhibitory post-synaptic currents (IPSCs) recorded from a principal cell in a Ctrl animal, 5 pulses of stimulation at a rate of 5 Hz. (C) Percent depression following light-evoked IPSCs in principal cells were not significantly different between groups for either the second or third light pulse (2-way RM, genotype p=0.3859, genotype-pulse interaction p=0.9978)(n=2 Ctrl, n=3 CST^{cre}/TrkB$^{flox/flox}$ mice). Average data are represented as mean ± SEM.

Supplemental Materials and Methods

Animals

Generation and characterization of BDNF-KIV mice was previously described (Sakata et al., 2009). BDNF-KIV mice used in this study were backcrossed to a C57Bl6/J background >12X. To selectively delete tropomyosin receptor kinase B (TrkB) from PV-positive interneurons we crossed TrkB$^{flox/flox}$ mice to mice expressing Cre recombinase from the endogenous Pvalb locus (B6;129P2-Pvalb$^{tm1(cre)Abr}$/J, referred to as PV^{cre}).

Chemoconvulsant induced seizures

Mice were treated either with 40 mg/kg pentylenetetrazol (PTZ) or 40 mg/kg kainic acid. Both drugs were dissolved in sterile saline. Following intraperitoneal (i.p.) injection, mice were subsequently observed for the latency to seize, seizure severity, and mortality as scored based on the modified Racine scale.

Motor skills testing

Behavioral assessments took place in Ctrl and PV^{cre}/TrkB$^{flox/flox}$ mice between 8-10 weeks of age. Open field assesments were conducted in an 18"x18" container, recorded from above using a "bird's eye" perspective. Mice were recorded for 30 minutes. Data was automatically processed using Topscan software (Cleversys Inc., Reston, VA). For accelerated rotarod testing, a four-lane accelerating rotarod (rod diameter: 3 cm; AccuRotor, AccuScan Instruments Inc., Columbus, OH) was used to assess motor skill acquisition. Rod velocity was set to increase from 0 to 40 rpm across the course of 5 min. Mice were placed in individual compartments, and subjected to six trials a day across 4 days. Latency to fall off the rod was automatically recorded by an automated beam break. Grip strength was measured by placing mice on a wire cage lid and recording latency to fall. Latency for each mouse was averaged across 2 trials.

Sharp wave discharge analysis

Analysis was conducted using custom Matlab scripts. Candidate SWD events were detected by first identifying local maxima and minima in the raw LFP (0-50 Hz) that exceeded 7 standard deviations above or below the mean LFP amplitude. Events less than 2.5 ms were discarded. Events were stored in a cell array, with each cell listing the time points at which the data was above the threshold for each event. This allowed for calculation of average length of the events, as well as the total event number. The peak-

triggered spectrogram was created by applying Morlet wavelet convolution to a raw LFP segment that occurred one second prior to and one second after a detected SWD event in a P32 $CST^{cre}/TrkB^{flox/flox}$ mouse.

Infusion of Channelrhodopsin virus targeting CST-expressing interneruons

General surgical procedures were followed as described in the main text. Stereotaxic infusion of non-diluted, Cre-dependent AAV virus was used to express Channnelrhodopsin-2 (ChR2) (AAV9.CAGGS.Flex.ChR2-tdTomato.WPRE.SV40, Catalog #AV-9-18917P, Penn Vector Core, Philadelphia, PA) to the P15-P18 cortex (+1.2 AP, 0.20 ML, and 1.275 DV) (Atasoy et al., 2008). A total volume of 350 nanoliters (nL) was infused, at a rate of 70 nL/min. Viral infusion occurred at least 9 d prior to recording, and recordings were started on or after P25.

In vitro light evoked IPSC recordings

Acute coronal slices of prefrontal cortex were made using cutting solution oxygenated with 95% O_2 and 5% CO_2 containing (in mM): 83 NaCl, 2.5 KCl, 26.2 $NaHCO_3$, 1 NaH_2PO_4, 22 glucose, 72 sucrose, 0.5 $CaCl_2$, and 3.3 $MgSO_4$. Slices were kept in the same solution and recovered in 42 degree for 40 minutes before recording. Patch pipettes were fabricated from borosilicate glass (N51A, King Precision Glass, Inc.) to a resistance of 2-5 mOhm using an upright puller (Narishige, model PC-10). The experiments were conducted in artificial cerebrospinal fluid (ACSF) contained (in mM): 125 NaCl, 3 KCl, 25 $NaHCO_3$, 1.25 NaH_2PO_4, 25 glucose, 2 $CaCl_2$, and 1 $MgCl_2$, and the pipettes were filled with internal solution containing (in mM): 110 $CsMeSO_4$, 10 CsCl, 10 HEPES, 10 Cs_4BAPTA, 5 QX-314, 0.1 Spermine, 4 Mg-ATP, 0.3 Na-GTP, 10 Phospocreatine, and pH to 7.3 with CsOH. The IPSCs were recorded in the presence of DNQX (10 uM, Abcam) and DL-AP5 (100 uM, Abcam) to block excitatory transmission. To evoke postsynaptic inhibitory currents the layer 2/3 pyramidal cells were held at -70mV and a brief train of light stimulation was delivered (5 pulses at 10 Hz, 1 ms laser duration) with various laser intensities near the field where cells are located using fiber optics (ThorLabs). The traces were collected every 30 s for 6 repetitions. All 6 traces were averaged for measurement and representation.

Supplemental References

Atasoy, D., Aponte, Y., Su, H.H., Sternson, S.M., 2008. A FLEX Switch Targets

Channelrhodopsin-2 to Multiple Cell Types for Imaging and Long-Range Circuit Mapping. J. Neurosci. 28, 7025–7030. doi:10.1523/JNEUROSCI.1954-08.2008

Sakata, K., Woo, N.H., Martinowich, K., Greene, J.S., Schloesser, R.J., Shen, L., Lu, B., 2009. Critical role of promoter IV-driven BDNF transcription in GABAergic transmission and synaptic plasticity in the prefrontal cortex. Proc Natl Acad Sci U S A 106, 5942–5947. doi:10.1073/pnas.0811431106